Journal of Biomaterials and Nanobiotechnology, **2012, 3, 342-352**
http://dx.doi.org/10.4236/jbnb.2012.33032 Published Online July 2012 (http://www.SciRP.org/journal/jbnb)

Acid-Functionalized Nanoparticles for Pretreatment of Wheat Straw

Leidy Peña[1], Myles Ikenberry[2], Keith L. Hohn[2], Donghai Wang[1*]

[1]Department of Biological and Agricultural Engineering, Kansas State University, Manhattan, USA; [2]Department of Chemical Engineering, Kansas State University, Manhattan, USA.
Email: *dwang@ksu.edu

Received April 15th, 2012; revised May 20th, 2012; accepted June 10th, 2012

ABSTRACT

Perfluoroalkylsulfonic (PFS) and alkylsulfonic (AS) acid-functionalized magnetic nanoparticles were synthesized, characterized, and then evaluated for their ability to hydrolyze hemicelluloses. The magnetic core was made of cobalt spinel ferrite and was coated with silica to protect it from oxidation. The silanol groups allowed surface chemical modification of the nanoparticles with the PFS and AS acid functionalities. Thermogravimetric analysis gave a total organic load of 12.6% and 32.5% (w/w) for AS and PFS nanoparticles, respectively. The surface sulfur content was calculated from XPS analysis as 1.37% and 1.93% for PFS and AS nanoparticles, respectively. Wheat straw samples were treated with the acid-functionalized nanoparticles at two different conditions: 80˚C for 24 h and 160˚C for 2 h. These experiments aimed to hydrolyze wheat straw hemicelluloses to soluble oligosaccharides. PFS nanoparticles solubilized significantly higher amounts of hemicelluloses (24.0% ± 1.1%) than their alkyl-sulfonic counterparts (9.1% ± 1.7%) at 80˚C, whereas the hydrothermolysis control solubilized 7.7% ± 0.8% of the original hemicelluloses in the sample. At 160˚C, PFS and AS nanoparticles gave significantly higher amounts of oligosaccharides (46.3% ± 0.4% and 45% ± 1.2%, respectively) than the control (35.0% ± 1.8%). The hemicelluloses conversion at 160˚C reached 66.3% ± 0.9% using PFS nanoparticles and 61.0% ± 1.2% using AS nanoparticles compared with the control experiment, which solubilized 50.9% ± 1.7% of hemicelluloses in the biomass.

Keywords: Acid-Functionalized Magnetic Nanoparticles; Biomass; Hemicelluloses; Hydrolysis

1. Introduction

Uncertainties in the oil supply and environmental problems associated with fossil fuels have motivated the search for other energy sources. Ethanol is a renewable energy source that can be used as transportation fuel. Global ethanol production increased 400% in the last decade. In 2009, 19 billion gallons of ethanol were produced worldwide [1]. In 2007, the USA government called for an increase in domestic biofuel production of up to 36 billion gallons by 2030 [2]. Production of ethanol as transportation fuel reached more than 13 billion gallons in 2010 in the US [3]. Currently, bio-ethanol is obtained from the alcoholic fermentation of monosaccharides derived from sugar-based and starchy crops [1]. These materials are also staple foods, so using them as fuel could strain the food supply. Alternatively, forest- and agricultural-derived biomass can be used for ethanol production after hydrolysis of their constitutive sugar polymers into monomers.

Lignocellulosic biomass comprises 38% - 50% cellulose, 23% - 32% hemicellulose, 15% - 22% lignin, and other minor components [4,5]. Cellulose fibers are polymers of β-1,4-linked glucopyranose units whose linear chains are glued with hemicelluloses and covered with a lignin sheath [6-8]. Hemicellulose is a heteropolymer of five- and six-carbon sugars that can be simultaneously fermented by modified strains [9]. Arabinoxylans are the most common hemicelluloses of the cell wall of cereal grains. The backbones of arabinoxylans are made of β-1, 4-D-xylopyranosyl units substituted with α-D-arabinofuranosyl units linked through the oxygens in the second or third position. Endosperm cell walls of wheat also have hemicelluloses rich in hexose units such as 1,4- and 1,3-linked β-D-glucan [10-12]. Xyloglucans are other hemicelluloses containing six carbon sugars; these hemicelluloses have β-1,4-linked D-glucopyranosyl backbones substituted with D-xylopyranose residues at the O-6 position. Xylose residues in xyloglucans can be further substituted with galactose or arabinose. These hemicelluloses can be found in the primary cell wall of plants; because of their chemical composition, xyloglucans can form strong associations with the cellulose fibrils [10,

*Corresponding author.

13-15]. Significant efforts have been made to obtain genetically engineered strains that can simultaneously metabolize hexose and pentose sugars into ethanol [10,11,16, 17]. The utilization of sugars from both hemicelluloses and celluloses could improve the economic feasibility of the production of cellulosic ethanol [18].

Pretreatment of lignocellulosic biomass is necessary to increase its susceptibility to enzymatic action. The most common pretreatment methods employ mineral acids and high temperatures to remove the lignin component [19-22]. Under these conditions, most of the sugars from hemicelluloses are degraded and can't be used for alcoholic fermentation [7,23-26]; moreover, substantial capital investment is required because corrosion-resistant materials need to be used. Neutralization, detoxification, and waste disposal are additional costs. Solid acids provide the catalytic properties of homogeneous acids with the advantage that they can be recovered from the reaction media by physical separation [27-29]. In previous studies, acid-functionalized mesoporous silicas have been employed for the conversion of starch and cellobiose to glucose [30,31]. Zeolites, Amberlyst-15, heteropolyacids, and sulfonated activated-carbon have been used for hydrolysis of cellulose into its glucose monomers [32,33]. Similar types of solid acids were used in the hydrolysis of hemicellulose and the recovery of xylose and arabinose sugars [34]. Dispersions of functionalized nanoparticles have similar catalylitic performance as their homogeneous counterparts [35,36]. Acid-functionalized nanoparticles could provide effective catalysis over a solid substrate such as biomass because their size is in the nanoscale. Furthermore, the magnetic nanoparticles can be recovered from the reaction media using a strong magnetic field [37-39]. The present work uses perfluoro-alkylsulfonic and alkyl-sulfonic acid-functionalized nanoparticles (PFS and AS) to catalyze the hydrolysis of hemicelluloses into oligosaccharides at two different temperatures.

2. Materials and Methods

2.1. Materials

Cobalt(II) chloride hexahydrate (99%), D-(+)-Cellobiose (98%), iron(II) chloride tetrahydrate (99.99%), 3-mercaptopropyltrimethoxysilane (MP-TMS) (95%), Nafion® SAC-13 (98%), methylamine (40% w/w, 98.5%), sodium dodecyl sulfate (98.5%), and tetraethylorthosilicate (TEOS) (99.999%) were purchased from Sigma-Aldrich Co. (St. Louis, MO). Ammonium hydroxide, toluene, and isopropanol (A.C.S. reagent) were purchased from Fisher Scientific (Pittsburgh, PA). Ethanol (95%) was purchased from Decon Laboratories (King of Prussia, PA). Hexafluoro (3-methyl-1-2-oxathiethane)-2,2-dioxide (HFP sultone) (95%) was purchased from SynQuest Labs (Alachua, FL). Wheat biomass was harvested from the Kansas State Agronomy Farm (Manhattan, KS) in November, 2008.

2.2. Synthesis of Acid-Functionalized Nanoparticles

2.2.1. Preparation of Silica-Coated Magnetic Nanoparticles (SiMNPs)

SiMNPs were synthesized according to methods previously described in the literature [38,40,41]. First, the magnetic core, which is composed of cobalt spinel ferrite ($CoFe_2O_4$), was synthesized by a microemulsion method. **Figure 1**, step 1, shows the procedure for preparation of SiMNPs. In a typical experiment, 500 ml of an aqueous solution was prepared containing 4 mmol of Cobalt(II) chloride hexahydrate, 5 mmol of iron(II) chloride, and 45 mmol of sodium dodecylsulfate (SDS). The solution was stirred at room temperature with a mechanical stirrer for 30 min and heated to 60˚C. Then, a warm methylamine solution (12% w/w) was added, and the mixture was stirred for 3 h. The nanoparticles were separated magnetically and washed 3 times using distilled water and twice with ethanol. The nanoparticles were dispersed in 100 ml of ethanol and stored at room temperature before coating with silica. The ethanol dispersion of nanoparticles was sonicated and stirred for 30 min, then 15 ml of the solution was added to a solution containing 500 ml isopropanol, 50 ml water, and 50 ml concentrated ammonium hydroxide. This solution was also sonicated under mechanical stirring for 1 h. A solution of 1 ml of tetraethylorthosilicate (TEOS) in 40 ml of isopropanol was added dropwise to the former solution. The mixture was sonicated under mechanical stirring for another 2 h. The nanoparticles were magnetically separated and washed with distilled water. Then the nanoparticles were dried in a vacuum oven at 45˚C for 48 h.

2.2.2. Acid Functionalization of the SiMNPs

Acid functionalization of SiMNPs was carried out following procedures reported in the literature [38]. **Figure 1**, steps 2 and 3, show the procedure for acid functionalization of SiMNPs. For the preparation of supported perfluoroalkylsufonic (PFS) acid-functionalized nanoparticles, dried SiMNPs (250 mg) were placed in a pressure bottle. Approximately 1 ml of HFP sultone and 20 ml of anhydrous toluene were poured into the bottle in a nitrogen glove bag. The pressure bottle was sealed and sonicated for 30 min. The mixture was stirred at 80˚C for 4 h in a water bath. The product (PFS nanoparticles) was magnetically separated and washed three times with 20 ml of anhydrous toluene. The nanoparticles were dried at 45˚C overnight in a vacuum oven. **Figure 1**, step 3, shows the procedure for preparation of supported alkylsufonic acid-functionalized (AS) nanoparticles. A solution containing

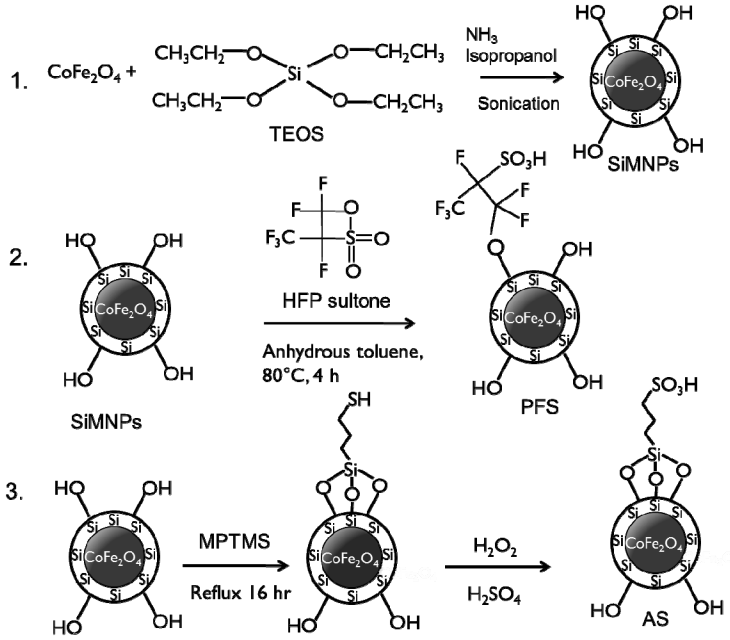

Figure 1. Step 1 depicts the silica-coating procedure. Cobalt iron oxide nanoparticles ($CoFe_2O_4$) are covered by a silica layer. The silica precursor is tetraethylorthosilicate (TEOS). The reaction is carried out in a basic media at room temperature under sonication and mechanical stirring. Step 2 shows the acid-functionalization procedure to obtain PFS nanoparticles. The reaction was carried out at 80˚C in a non-polar medium for 4 h. Step 3 shows a scheme of the acid functionalization of SiMNPS to obtain AS. Mercaptopropyltrimethoxysilane (MPTMS) was used as the precursor of the propylsulfonic acid grafted onto SiMNPs. An oxidation step is required to oxidize –SH groups to –SO_3H.

1 ml of MPTMS, 10 ml of ethanol, and 10 ml of distilled water was prepared, and then 1 g of SiMNPs was added. The mixture was sonicated for 60 min and refluxed overnight. The product was recovered magnetically and washed four times with 10 ml of water. To oxidize the mercapto groups in the nanoparticles, a blend of 10 ml of 30% hydrogen peroxide, 10 ml of water, and 10 ml of methanol was added to the nanoparticles. This mixture was kept under static conditions and at room temperature for three days. The product from the oxidation step was recovered magnetically and washed three times with 20 ml water. The particles were reacidified with 20 ml of 2 M H_2SO_4, washed three times with distilled water, and dried at 45˚C for 48 h.

2.3. Characterization of Acid-Functionalized Nanoparticles

Transmission electron microscope (TEM) images were used to estimate the size and size distribution of the nanoparticles. A model CM100 TEM (FEI Company, Hillsboro, OR) equipped with an AMT digital image capturing system was operated at 100 kV. The images were taken under both dispersed and dried conditions. For dispersed solutions, the nanoparticles were absorbed for approximately 30 s at room temperature onto Formvar/carbon-coated, 200-mesh copper grids (Electron Microscopy Sciences, Fort Washington, PA), then viewed by TEM. The mean size of the nanoparticles was estimated using the software ImageJ, available from the National Institute of Health. Particle analysis of aggregates was done on a particles size analyzer (LTS-150, LECO Corp., St Joseph, MI).

Fourier transform infrared (FTIR) spectra were used to investigate the chemical bonds presented on the nanoparticles. Spectroscopy-grade KBr and samples were dried at 45˚C for 48 h, and then prepared by mixing 2 mg of sample with 200 mg of KBr. The measurement was carried out between wave numbers 400 - 4000 cm^{-1}, with detectors at 4 cm^{-1} resolution and 32 scans per sample using a Thermo Nicolet NEXUSTM 870 infrared spectrometer with a ZnSe window. An OMNIC software program (Thermo Electron Corporation, Madison, WI) was used to determine the peak positions and intensities.

X-ray photoelectron spectroscopy (XPS) was used to analyze the surface functional groups covalently attached to SiMNP. The data were obtained with a PerkinElmer PHI 5400 (Waltham, MA) electron spectrometer using acrochromatic AlKα radiation (1486.6 eV). Spectra were obtained under vacuum pressure around 2.0×10^{-8} Torr. XPS binding energies were measured with a precision of 0.1 eV. The analyzer pass energy was 17.9 eV, with a contact time of 50 ms. The nanoparticles were sputtered for 2 min before analysis.

Thermogravimetric analysis (TGA) was used to count the organic load over the nanoparticles after immobilization. The TGA was carried out in a PerkinElmer Pyris1 TGA (Norwalk, CT). About 5 mg of each sample was placed in the pan and heated from 30˚C to 700˚C at a rate of 20˚C/min under a nitrogen atmosphere.

2.4. Biomass Pretreatment

The capacity of PFS and AS nanoparticles to hydrolyze hemicellulose was evaluated at two temperatures, 80˚C and 160˚C. For the experiments at 80˚C, 2.5% (w/w) wheat straw and 1.5% (w/w) catalyst were used. The total weight of the slurry was 26 g. The hydrolysis was carried out in pressure bottles for 24 h. All bottles were sealed to avoid mass loss. For the experiments at 160˚C, 2.5% (w/w) wheat straw samples were pretreated with 0.25% (w/w) AS or PFS nanoparticles for 2 h. In this case, the hydrolysis was carried out in a 600 ml pressure reactor (Model 4544; Parr Instrument Co., Moline, IL). An experimental control was also run at both temperatures with the biomass sample under the same conditions but without catalyst. After pretreatment, the solid fraction was separated from the slurry using a 200-mesh sieve. The nanoparticles were magnetically separated from the liquid fraction, which was analyzed for sugar content.

2.5. Analytical Methods

Structural carbohydrates and lignin content of wheat straw were analyzed following the NREL LAP procedure TP-510-42618 [42]. After the biomass pretreatment with AS, PFS, and without catalyst (control), the total amount of carbohydrates in the liquid fraction was determined following the NREL LAP procedure TP-510-42623 [43]. This method hydrolyzes the oligosaccharides in the liquid fraction into their monomer constituents. Sulfuric acid (72% w/w) was used to bring the acid concentration of the liquid fraction to 4% (w/w). The samples were placed in pressure bottles and sealed. The bottles were autoclaved at 121˚C for 1 h, then the samples were neutralized with $CaCO_3$, filtered, and analyzed by HPLC. The sugars were quantified using RCM-Ca+2 and RPM-Pb+2 monosaccharide columns (300 × 7.8 mm; Phenomenex, Torrance, CA) and a refractive index detector. Samples were run at 80˚C and 0.6 ml/min with deionized water. Recovered hemicellulose was counted as the amount of D-(+)-xylose, and D-(+)-arabinose derived from the initial hemicellulose fraction in the biomass samples before pretreatment. Hemicellulose yield (%) was calculated as the ratio of total hemicellulose sugars detected in the liquid fraction after pretreatment to the initial amount of hemicelluloses in the biomass before pretreatment.

3. Results and Discussion

3.1. Characterization of Acid-Functionalized Nanoparticles

The TEM images were taken under both dispersed and dried conditions. Images (a) and (b) in **Figure 2** were taken over $CoFe_2O_4$ particles dispersed in ethanol. Ethanoldispersed nanoparticles were sonicated for 60 min before TEM analysis. Dispersed $CoFe_2O_4$ nanoparticles can be seen in **Figure 2(a)**. $CoFe_2O_4$ aggregates were also observed in ethanol solution (**Figure 2(b)**). Monodispersed nanoparticles had an average diameter of 7.6 nm with a standard deviation of 2.7 nm based on a total of 120 particles. The size of the aggregates measured the particle analyzer was equal to 2.3 μm with a standard deviation of 0.3 μm. The silica-coating process is sensitive to the TEOS addition rate. When the TEOS was added at high rates, the mean size and standard deviation of the silicacoated nanoparticles were 653 nm and 56 nm, respectively, based on total of 226 nanoparticles (**Figure 2(c)**). A TEM image of SiMNPs obtained after dropwise addition of the TEOS is shown in **Figure 2(d)**. The mean size of SiMNPs was 3.5 nm with a standard deviation of 1.6 nm based on 629 nanoparticles. The mean size of SiMNPs aggregates was 2.2 μm with a standard deviation of 0.3 μm. Acid functionalization changed the dispersability of the nanoparticles because larger aggregates were found after this step. The material functionalized with PFS acid groups showed a bimodal distribution; the smaller distribution could be attributed to silica-coated

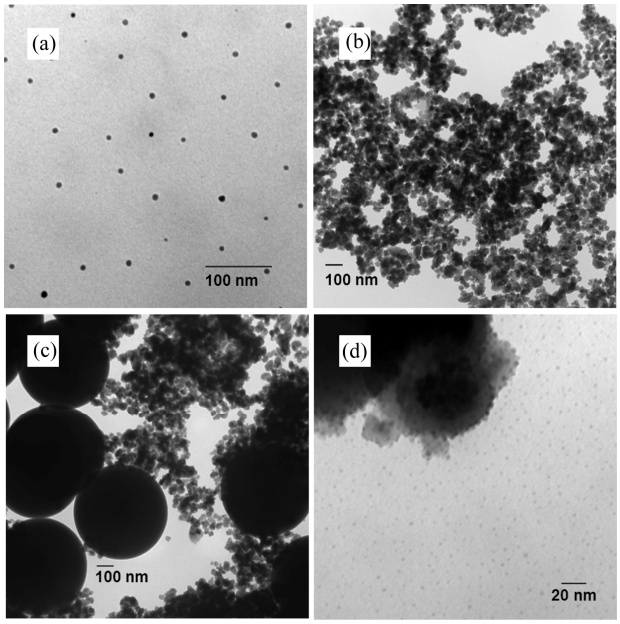

Figure 2. TEM images of (a) cobalt iron oxide ($CoFe_2O_4$) nanoparticles; (b) $CoFe_2O_4$ aggregates of nanoparticles; (c) SiMNPs synthesized at high addition rates of TEOS; and (d) SiMNPs synthesized at low addition rates of TEOS.

iron oxide that escaped the functionalization. The smaller material had a mean of 2.3 (±0.1) µm, which is the same as that obtained for silica-coated iron oxide aggregates. The functionalization with PFS had promoted the formation of larger aggregates with a mean size of 74.0 (±4.1) µm. AS nanoparticles also showed a bimodal distribution with mean diameter of 13. (±2.5) µm for the larger aggregates and mean diameter of 0.8 (±0.1) µm for the smaller aggregates.

FTIR spectra for acid-functionalized nanoparticles are shown in **Figure 3**. The broad band in the wavelength 500 - 600 cm^{-1} appears in all the spectra. This band has been associated to Fe-O bonds [44,45]. The bands at 820 and 960 cm^{-1} in SiMNPs, AS, and PFS spectra have been attributed to the stretching vibrations of Si–O–Si and Si–O–H groups [46]. Similarly, a broad band at 1120 cm^{-1} from the Si–O bond appears in all these spectra [47]. The peak at 1370 cm^{-1} has been assigned to the O=S=O stretching vibrations [48-51]. The peaks at 1425 cm^{-1} in the spectra of AS and PFS nanoparticles have been attributed to undissociated SO_3H groups [48,50]. The peaks at 1080, 1150, and 1190 cm^{-1} in the spectrum of PFS nanoparticles have been assigned to the C-F bond [52-54]. The results from FTIR analysis showed that all of the nanoparticles had the functional groups expected.

XPS profiles for PFS and AS functionalized nanoparticles were used to analyze their atomic concentration (**Figure 4**). A peak at 104 - 108 eV was observed for both acid-functionalized nanoparticles. This peak is associated with silicon bonds from the silica layer that covers the $CoFe_2O_4$ nanoparticles [51,55]. The peaks associated with carbon, silicon, and sulfur were observed in the AS spectrum. The surface composition of both PFS and AS nanoparticles is shown in **Table 1**. For AS, the C/Si theoretical value was calculated from the molecular formula of the propylsulfonic acid attached to the silica surface as 3. The C/Si ratio of 3.4 from the XPS experiment agrees with the theoretical value. The C/S ratio of 26.6 was much larger than the theoretical value, which is also 3.0. The large amount of carbon with respect to sulfur suggests that the loss of the sulfonic acid groups might have occurred during the synthesis procedure. The peaks that correspond to F, O, C, S, and Si were found in the XPS profiles for PFS nanoparticles. As in the AS case, the C/S ratio of 10.4 was greater than the theoretical value of 3.0. The large amount of carbon also suggests the loss of the sulfonic acid group during the synthesis procedure; however, the ratio of fluorine to carbon (0.8) was lower than expected (3.0), which indicates that the acid sulfonic group leached out along with other fluorine atoms of the HFP sultone moieties.

The thermal decomposition scans of the nanoparticles before and after acid functionalization were used to evaluate the thermal stability of the nanoparticles and

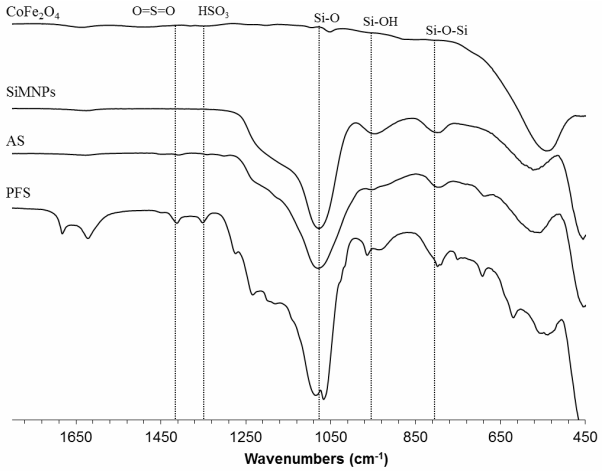

Figure 3. FTIR spectra of $CoFe_2O_4$, SiMNPs, AS-SiMNPs, and PFS-SiMNPs after synthesis. All the samples were dried at 45˚C under vacuum before taking the spectra.

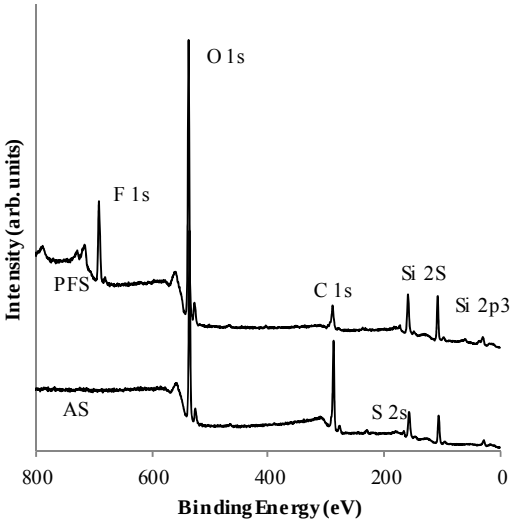

Figure 4. XPS profiles of PFS and AS nanoparticles.

Table 1. Atomic concentration and organic load of the acid-functionalized nanoparticles.

	Atomic concentration[a] (%)					Organic load[b] (%)	mmol H^+/g^c
	F	O	C	S	Si		
PFS	11.52	47.94	14.2	1.37	24.36	30.4	0.13
AS	-	31.61	51.28	1.93	15.19	12.6	0.07

[a]From XPS analysis; [b]From TGA analysis; [c]Calculated.

their total organic loading (**Figure 5**). The DTA curves show that the drying step occurred before the samples reached 150˚C. SiMNPs had absorbed more water than the acid-functionalized nanoparticles. The moisture content of SiMNPs, AS, and PFS nanoparticles was 3.9%, 2.6%, and 2.6%, respectively. The incorporation of alkylsulfonic and perfluoroalkylsulfonic acids groups increased

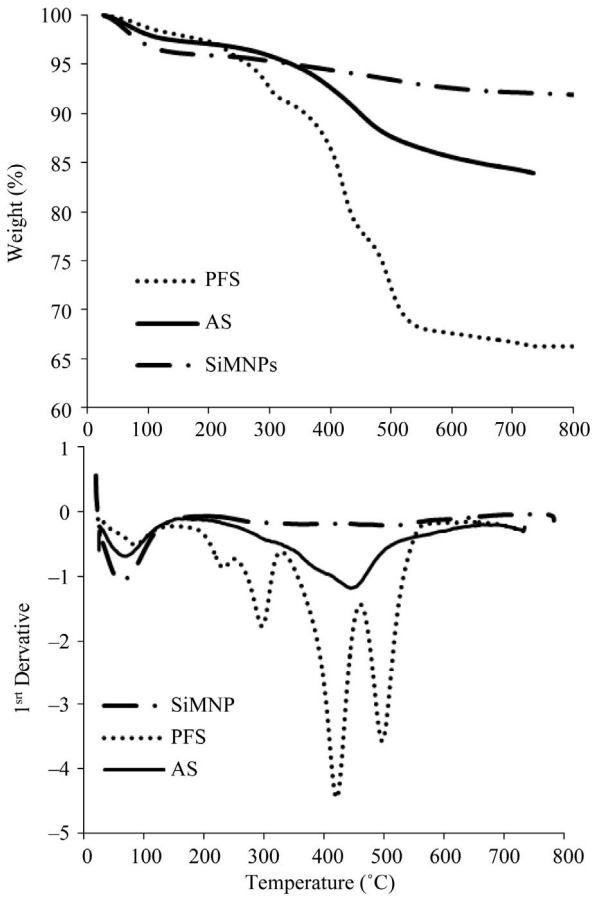

Figure 5. TG/DTA profiles of SiMNP, PFS, and AS functionalized nanoparticles.

the hydrophobicity of the nanoparticles. Similar results were found during functionalization of silica with perfluoroalkylsulfonic acid [51]. An increase in the hydrophobic properties of the nanoparticles can affect their dispersability in the biomass slurry and could promote aggregation of nanoparticles, thus reducing the available area for the reaction. The TGA profile of SiMNPs showed a total weight loss of 4.2% during heating from 150˚C to 800˚C. The weight loss between 150˚C and 400˚C was 1.7% and it has been attributed to bound water. The weight loss at temperatures higher than 400˚C was measured as 2.5% and it has been explained as the weight lost due to a ferrite crystallization process [44,56]. PFS and AS nanoparticles showed similar thermal stabilities; when heated to 450˚C, PFS nanoparticles lost 22% of their weight, or about 60% of their original organic content; AS lost 10% of their weight, or about 55% of their original organic content. The first derivative profile for PFS nanoparticles shows four peaks at 225˚C, 292˚C, 417˚C, and 492˚C, which indicates that the perfluoroalkylsulfonic acid group splits into smaller moieties. The sulfonic acid groups and the CF2-chains decompose at different temperatures [51]. The first derivative profile for AS nanoparticles shows a main peak at 437˚C that corresponds to the alkyl-sulfonic acid. The left shoulder on this peak could be attributed to mercapto-propyl groups that were not completely oxidized to the sulfonic acid [57]. The total organic content was counted as the total mass lost between 150˚C and 600˚C; these values can be seen in **Table 1** along with the number of acid sites on the nanoparticles. The hydronium ion concentration per mass of catalyst was calculated from the values of total organic content on the nanoparticles and the surface sulfur concentration.

3.2. Biomass Pretreatment

Table 2 shows the biomass composition on a dry mass basis, and the total hemicellulose sugars recovered at 80˚C and 160˚C from wheat straw are shown in **Figure 6**.

At temperatures as low as 80˚C, solubilization of hemicellulose rather than cellulose hydrolysis is expected [8]. The amount of sugars solubilized (24.0% ± 1.1%) at 80˚C in the presence of PFS nanoparticles was greater

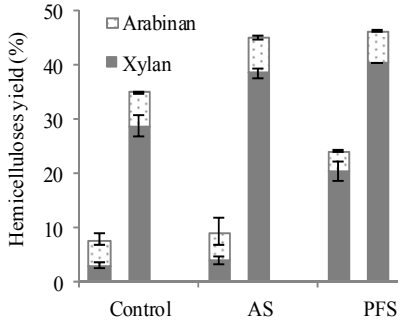

Figure 6. Wheat straw hemicelluloses recovered after pretreatment with PFS and AS acid-functionalized nanoparticles. The left columns correspond to results of the experiments carried out at 80˚C for 24 h with a catalyst load of 1.5% and biomass load of 2.5%. Results of the experiments carried out at 160˚C for 2 h with a catalyst load of 0.25% and biomass load of 2.5% are shown in the right columns. The error bars represent the standard errors of two replicate experiments.

Table 2. Whole biomass composition.

Biomass constituents	Wheat straw
95% ethanol extractives	16.4 ± 2.5
Acid-insoluble ash (%)	3.6 ± 1.0
Acid-soluble lignin (%)	0.8 ± 0.1
Acid-insoluble lignin (%)	15.3 ± 0.6
Total lignin (%)	16.1 ± 0.6
Xylan (%)	17.2 ± 2.1
Glucan (%)	33.5 ± 3.1
Arabinan (%)	1.7 ± 0.4

than the sugars released from the control (7.7% ± 0.8%); but the amount of hemicelluloses recovered with AS (9.1% ± 1.7%) was not significantly different from the control. PFS experiments used 2 mmol H^+/L based on the values obtained for organic content and sulfur atomic concentration; this is equivalent to using 0.02% (w/w) sulfuric acid solutions. By a similar calculation, the load of AS nanoparticles provides 1.02 mmol H^+/L, which is equivalent to using 0.01% (w/w) sulfuric acid solutions. Hemicellulose yield of 20% can be considered moderate because low temperature and acidity levels were used. Complete (100%) hemicellulose solubilization requires temperatures higher than 160˚C using 1% sulfuric acid [8]. Previous work reported that complete xylan solubilization was reached at 130˚C using 3% (w/w) sulfuric acid solutions for 4 h [58]. Higher temperatures have been used (180˚C - 220˚C) for hemicellulose hydrolysis with acid concentrations between 0% to 0.1% sulfuric acid (w/w) [59-61].

Very few monosaccharides were obtained after pretreatment of biomass with PFS or AS nanoparticles. PFS and AS solubilized the xylan fraction into its monomeric form at very low levels: 3.5% ± 0.1%, 1.0% ± 0.2% at 80˚C. Xylose monomer units were not detected in the solution for the control experiment. In the experiments carried out at 160˚C, only 0.3% and 1.2% of the original xylan was found in the solution as xylose for PFS and AS nanoparticles, respectively. From the initial arabinan, 49.5% ± 2.1% and 57.9% ± 11.2% was found as arabinose monomer in the pretreatment liquor of AS and PFS nanoparticles. In the control experiment, 36.0% ± 1.6% of arabinan was hydrolyzed to the monomeric form. These results agree with previous findings in which acid-functionalized amorphous carbon was used to hydrolyze cellulose, the yield of monomers was only 4%, and most of the sugars obtained were in oligomeric form [49]. About 30% monomers yield was obtained from loblolly pine hemicelluloses using 1% sulfuric acid at 150˚C and 60% at 200˚C [62]. At 160˚C, the low percentage of xylose found in the solution could be explained by degradation of the xylose units to other products such as furfural and formic acid [63-67]; in this experiment, 16.0% ± 0.2%, 20.0% ± 1.3%, and 15.7% ± 1.2% of the original xylan was found in solution as furfural for AS, PFS, and control, respectively (**Figure 7**). Formic acid was also found in the pretreatment liquor, but it may have been a degradation product of either cellulose or xyloglucans. The results of this paper agree with the hemicellulose hydrolysis models proposed in the literature [59,68-71]. These models suggest that either hemicelluloses or xylan are made of two different fractions that are hydrolyzed at different rates, one slow and one fast. In the present work, the fast-hydrolyzing fraction of hemicellulose is degraded to decomposition products, and that is why very few

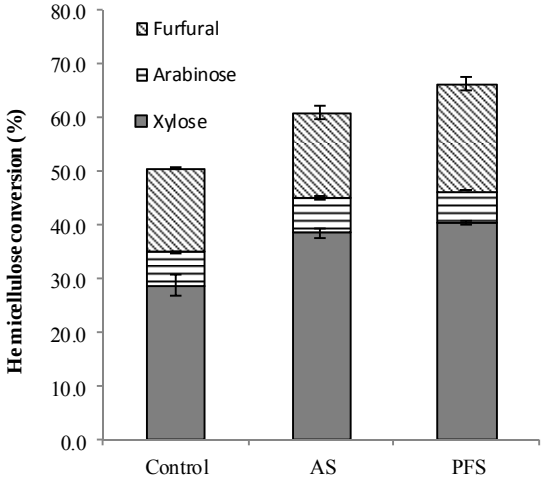

Figure 7. Wheat straw hemicelluloses solubilized after pretreatment with PFS and AS acid-functionalized nanoparticles. The pretreatment was carried out at 160˚C for 2 h with a catalyst load of 0.25% and biomass load of 2.5%. The error bars represent the standard errors of two replicate experiments.

monomers were found in the pretreatment liquor. The slow-hydrolyzing fraction is found in solution as oligomers or remains in the non-hydrolyzed solid fraction.

In the experiments performed at high temperature, a 0.25% (w/w) catalyst load was used; the PFS and AS nanoparticle dispersions are equivalent to using 0.003% and 0.002% (w/w) sulfuric acid solutions, respectively. The total hemicellulose (oligosaccharides and monosaccharides) recovered from wheat straw at 160˚C reached 46.3% ± 0.4% and 45.0% ± 1.2% using PFS and AS, respectively. The control experiment recovered 35.0% ± 1.8% of the original hemicellulose in the wheat straw sample. Most of the sugars found in solution came from the xylan fraction 38.6% ± 0.9% and 40.4% ± 0.2% using AS and PFS, respectively. Hemicellulose solubilization could have been affected by the buffering effect of the biomass, which has been said could reduce 1% (w/w) acid concentration in half [8]. Low acid levels are frequently used along with high temperatures; hemicellulose conversions of up to 97% (w/w) have been reported when using 0.1% (w/w) sulfuric acid at 180˚C, but still more than 50% was oligomers of hemicellulose [72]. In a another study, 96% (w/w) conversion of hemicellulose was obtained with 0.8% (w/v) sulfuric acid from yellow poplar sawdust at 175˚C [61]. PFS and AS nanoparticles converted 66.3% ± 1.7% and 61.0% ± 1.2% of the hemicelluloses at acid levels 50 and 400 fold lower than those acid sulfuric solutions at 160˚C.

PFS and AS nanoparticles gave similar amounts of recovered hemicellulose; and both catalysts gave more sugars than the control. A better performance of PFS nanoparticles was expected because perfluorosulfonic

acids are known as superacids and can be more acidic than sulfuric acid [27,48,73]. The acid strength of these acids has been explained by the electron-withdrawing properties of the Fluorine atoms [74], but the leveling effect of water could have an effect on the catalytic activity of PFS nanoparticles [74]. Nanoparticles functionalized with alkyl-sulfonic acid show a significant improvement on hemicelluloses solubilization when using 160˚C instead of 80˚C, although the acid loading for this catalyst was relatively low. Similar acid capacity was reported previously for propyl-sulfonic acid-functionalized materials [38]. Low catalytic activity also could have been a consequence of the low water affinity observed for this catalyst in TGA experiments. These results agree with the findings of Van Rhijn *et al*. [75], who synthesized mesoporous silicas functionalized with propylsulfonic acid and obtained moisture contents of less than 1%. The aggregation of both PFS and AS nanoparticles also could have an effect on their capacity to hydrolyze hemicelluloses due to a considerable reduction of their surface area; however, the attachment of PFS and AS acid functions could have stabilized the acid and allowed moderate levels of hemicellulose hydrolysis compared with sulfuric acid solutions of similar acid strength.

4. Conclusion

Acid-functionalized magnetic nanoparticles were synthesized as catalysts for pretreatment and hydrolysis of lignocellulosic feedstock. TEM images confirmed that the synthesis of cobalt spinel ferrite yielded particles with diameters less than 10 nm. Coating the cobalt spinel ferrite particles did not significantly change the size distribution of the nanoparticles, although some particles agglomerated upon coating. FTIR and XPS spectra confirmed the covalent bonding between the magnetic core and the silica layer and the presence of sulfonic acid groups following functionalization. Analysis of sugars in the liquid fraction after pretreatment revealed a significant amount of oligosaccharides compared with the hydro-thermolysis when using PFS or AS nanoparticles at 160˚C. The acid-functionalized nanoparticles broke down the non-soluble polysaccharides into oligomeric forms.

5. Acknowledgements

This project is supported by the NSF award CNET-1033538 and the NSF EPSCoR Kansas Center for Solar Energy Research. This material is also based upon work supported by NSF Grant # 0903701: “Integrating the Socioeconomic, Technical, and Agricultural Aspects of Renewable and Sustainable Biorefining Program awarded to Kansas State University.” Contribution number 12-367-J from the Kansas Agricultural Experiment Station.

REFERENCES

[1] Renewable Fuels Association, “2010 Ethanol Industry Outlook,” 2010.

[2] Senate and House of Representatives of the United States of America in Congress, “Energy Indepence and Security Act,” 2007.

[3] Office of the Biomass Program, “Biomass: Multi-Year Program Plan, U.S. DOE,” 2010.

[4] S. Iborra, A. Corma and G. Huber, “Synthesis of Transportation Fuels from Biomass: Chemistry, Catalysts, and Engineering,” *Chemical Reviews*, Vol. 106, No. 9, 2006, pp. 4044-4098. doi:10.1021/cr068360d

[5] C. E. Wyman and B. J. Goodman, “Biotechnology for Production of Fuels, Chemicals, and Materials from Biomass,” *Applied Biochemistry and Biotechnology*, Vol. 39-40, No. 1, 1993, pp. 41-59. doi:10.1007/BF02918976

[6] R. Preston, “Fibrillar Units in the Structure of Native Cellulose,” *Discussions of the Faraday Society*, Vol. 11, No. 11, 1951, pp. 165-170. doi:10.1039/df9511100165

[7] O. Bobleter, “Hydrothermal Degradation of Polymers Derived from Plants,” *Progress in Polymer Science*, Vol. 19, No. 5, 1994, pp. 797-841. doi:10.1016/0079-6700(94)90033-7

[8] J. D. McMillan, “Pretreatment of Lignocellulosic Biomass,” In: M. E. Himmel, J. O. Baker and R. P. Overend, Eds., *Enzymatic Conversion of Biomass for Fuels Production*, American Chemical Society, 1994, pp. 292-294. doi:10.1021/bk-1994-0566.ch015

[9] N. Rodrussamee, N. Lertwattanasakul, K. Hirata, S. Limtong and T. Kosaka, “Growth and Ethanol Fermentation Ability on Hexose and Pentose Sugars and Glucose Effect Under various Conditions in Thermotolerant Yeast Kluyveromyces Marxianus,” *Applied Microbiology and Biotechnology*, Vol. 90, No. 4, 2011, pp. 1573-1586. doi:10.1007/s00253-011-3218-2

[10] F. M. Girio, C. Fonseca, F. Carvalheiro, L. C. Duarte and S. Marques, “Hemicelluloses for Fuel Ethanol: A Review,” *Bioresource Technology*, Vol. 101, No. 13, 2010, pp. 4775-4800. doi:10.1016/j.biortech.2010.01.088

[11] L. Olsson, H. R. Soerensen, B. P. Dam, H. Christensen and K. M. Krogh, “Separate and Simultaneous Enzymatic Hydrolysis and Fermentation of Wheat Hemicellulose with Recombinant Xylose Utilizing Saccharomyces Cerevisiae,” *Applied Biochemistry and Biotechnology*, Vol. 129, No. 1-3, 2006, pp. 117-129. doi:10.1385/ABAB:129:1:117

[12] A. Bacic and B. Stone, “A (1 → 3)-Linked and (1 → 4)-Linked Beta-D-Glucan in the Endosperm Cell-Walls of Wheat,” *Carbohydrate Research*, Vol. 82, No. 2, 1980, pp. 372-377. doi:10.1016/S0008-6215(00)85713-4

[13] V. Menon, G. Prakash and M. Rao, “Enzymatic Hydrolysis and Ethanol Production Using Xyloglucanase and Debaromyces Hansenii from Tamarind Kernel Powder: Galactoxyloglucan Predominant Hemicellulose,” *Journal of Biotechnology*, Vol. 148, No. 4, 2010, pp. 233-239. doi:10.1016/j.jbiotec.2010.06.004

[14] R. de Vries and J. Visser, “Aspergillus Enzymes Involved

in Degradation of Plant Cell Wall Polysaccharides," *Microbiology and Molecular Biology reviews*, Vol. 65, No. 4, 2001, pp. 497-522. doi:10.1128/MMBR.65.4.497-522.2001

[15] J. Vincken, W. York, G. Beldman and A. Voragen, "Two General Branching Patterns of Xyloglucan, XXXG and XXGG," *Plant Physiology*, Vol. 114, No. 1, 1997, pp. 9-13. doi:10.1104/pp.114.1.9

[16] A. Matsushika, H. Inoue, K. Murakami, O. Takimura and S. Sawayama, "Bioethanol Production Performance of Five Recombinant Strains of Laboratory and Industrial Xylose-Fermenting Saccharomyces Cerevisiae," *Bioresource Technology*, Vol. 100, No. 8, 2009, pp. 2392-2398. doi:10.1016/j.biortech.2008.11.047

[17] J. Song and D. Wei, "Production and Characterization of Cellulases and Xylanases of Cellulosimicrobium Cellulans Grown in Pretreated and Extracted Bagasse and Minimal Nutrient Medium M9," *Biomass Bioenergy*, Vol. 34, No. 12, 2010, pp. 1930-1934. doi:10.1016/j.biombioe.2010.08.010

[18] C. Q. Zhang, W. Qi, F. Wang, Q. Li and R. X. Su, "Ethanol from Corn Stover using SSF: An Economic Assessment," *Energy Sources Part B*: *Economics*, *Planning and Policy*, Vol. 6, No. 2, 2011, pp. 136-144.

[19] D. Y. Corredor, X. S. Sun, J. M. Salazar, K. L. Hohn and D. Wang, "Enzymatic Hydrolysis of Soybean Hulls using Dilute Acid and Modified Steam-Explosion Pretreatments," *Journal of Biobased Materials and Bioenergy*, Vol. 2, No. 1, 2008, pp. 43-50. doi:10.1166/jbmb.2008.201

[20] E. Viola, F. Nanna, E. Larocca, M. Cardinale, D. Barisano and F. Zimbardi, "Acid Impregnation and Steam Explosion of Corn Stover in Batch Processes," *Industrial Crops and Products*, Vol. 26, No. 2, 2007, pp. 195-206. doi:10.1016/j.indcrop.2007.03.005

[21] U.S. Department of Energy, "Concentrated Acid Hydrolysis," 2006. http://www1.eere.energy.gov/biomass/printable_versions/concentrated_acid.html

[22] Y. Lee and S. Kim, "Diffusion of Sulfuric Acid within Lignocellulosic Biomass Particles and Its Impact on Dilute-Acid Pretreatment," *Bioresource Technology*, Vol. 83, No. 2, 2002, pp. 165-171. doi:10.1016/S0960-8524(01)00197-3

[23] N. S. Mosier, C. M. Ladisch and M. R. Ladisch, "Characterization of Acid Catalytic Domains for Cellulose Hydrolysis and Glucose Degradation," *Biotechnology and Bioengineering*, Vol. 79, No. 6, 2002, pp. 610-618. doi:10.1002/bit.10316

[24] K. Cejpek, J. Velisek and O. Novotny, "Formation of Carboxylic Acids during Degradation of Monosaccharides," *Czech Journal of Food Science*, Vol. 26, No. 2, 2008, pp. 113-131.

[25] J. Delgenes, "Effects of Lignocellulose Degradation Products on Ethanol Fermentations of Glucose and Xylose by Saccharomyces Cerevisiae, Zymomonas Mobilis, Pichia Stipitis, and Candida Shehatae," *Enzyme and Microbial Technology*, Vol. 19, No. 3, 1996, pp. 220-225. doi:10.1016/0141-0229(95)00237-5

[26] J. M. Oliva, M. J. Negro and F. Saez, "Effects of Acetic Acid, Furfural and Catechol Combinations on Ethanol Fermentation of Kluyveromyces Marxianus," *Process Biochemistry*, Vol. 41, No. 5, 2006, pp. 1223-1228. doi:10.1016/j.procbio.2005.12.003

[27] A. Corma and H. Garcia, "Silica-Bound Homogeneous Catalysts as Recoverable and Reusable Catalysts in Organic Synthesis." *Advanced Synthesis & Catalysis*, Vol. 348, No. 12-13, 2006, pp. 1391-1412. doi:10.1002/adsc.200606192

[28] M. A. Harmer, Q. Sun, A. J. Vega, W. E. Farneth, A. Heidekum and W. F. Hoelderich, "Nafion Resin-Silica Nanocomposite Solid Acid Catalysts. Microstructure-Processing-Property Correlations," *Green Chemistry*, Vol. 2, No. 1, 2000, pp. 7-14. doi:10.1039/a907892d

[29] M. Yurdakoc, M. Akcay, Y. Tonbul and K. Yurdakoc, "Acidity of Silica-Alumina Catalysts by Amine Titration using Hammett Indicators and FT-IR Study of Pyridine Adsorption," *Turkish Journal of Chemistry*, Vol. 23, No. 3, 1999, pp. 319-327.

[30] J. A. Bootsma and B. H. Shanks, "Cellobiose Hydrolysis Using Organic-Inorganic Hybrid Mesoporous Silica Catalysts," *Applied Catalysis A-General*, Vol. 327, No. 1, 2007, pp. 44-51.doi:10.1016/j.apcata.2007.03.039

[31] P. L. Dhepe, M. Ohashi, S. Inagaki, M. Ichikawa and A. Fukuoka, "Hydrolysis of Sugars Catalyzed by Water-Tolerant Sulfonated Mesoporous Silicas," *Catalysis Letters*, Vol. 102, No. 3-4, 2005, pp. 163-169. doi:10.1007/s10562-005-5850-x

[32] A. Onda, T. Ochi and K. Yanagisawa, "Selective Hydrolysis of Cellulose into Glucose Over Solid Acid Catalysts," *Green Chemistry*, Vol. 10, No. 10, 2008, pp. 1033-1037. doi:10.1039/b808471h

[33] K. Shimizu, H. Furukawa, N. Kobayashi, Y. Itaya and A. Satsuma, "Effects of Bronsted and Lewis Acidities on Activity and Selectivity of Heteropolyacid-Based Catalysts for Hydrolysis of Cellobiose and Cellulose," *Green Chemistry*, Vol. 11, No. 10, 2009, pp. 1627-1632. doi:10.1039/b913737h

[34] P. Dhepe and R. Sahu, "A Solid-Acid-Based Process for the Conversion of Hemicellulose," *Green Chemistry*, Vol. 12, No. 12, 2010, pp. 2153-2156. doi:10.1039/c004128a

[35] A. Bell, "The Impact of Nanoscience on Heterogeneous Catalysis," *Science*, Vol. 299, No. 5613, 2003, pp. 1688-1691. doi:10.1126/science.1083671

[36] V. Polshettiwar and R. Varma, "Green Chemistry by Nano-Catalysis," *Green Chemistry*, Vol. 12, No. 5, 2010, pp. 743-754. doi:10.1039/b921171c

[37] M. Zhang, B. L. Cushing and C. J. O'Connor, "Synthesis and Characterization of Monodisperse Ultra-Thin Silica-Coated Magnetic Nanoparticles," *Nanotechnology*, Vol. 19, No. 8, 2008, pp. 1-5. doi:10.1088/0957-4484/19/8/085601

[38] C. S. Gill, B. A. Price and C. W. Jones, "Sulfonic Acid-Functionalized Silica-Coated Magnetic Nanoparticle Catalysts." *Journal of Catalysis*, Vol. 251, No. 1, 2007, pp. 145-152. doi:10.1016/j.jcat.2007.07.007

[39] P. D. Stevens, J. Fan, H. M. R. Gardimalla, M. Yen and Y.

Gao, "Superparamagnetic Nanoparticle-Supported Catalysis of Suzuki Cross-Coupling Reactions." *Organic Letters*, Vol. 7, No. 11, 2005, pp. 2085-2088. doi:10.1021/ol050218w

[40] N. T. S. Phan and C. W. Jones, "Highly Accessible Catalytic Sites on Recyclable Organosilane-Functionalized Magnetic Nanoparticles: An Alternative to Functionalized Porous Silica Catalysts," *Journal of Molecular Catalysis A*: *Chemical*, Vol. 253, No. 1-2, 2006, pp. 123-131. doi:10.1016/j.molcata.2006.03.019

[41] A. J. Rondinone, A. C. S. Samia and Z. J. Zhang, "Superparamagnetic Relaxation and Magnetic Anisotropy Energy Distribution in $CoFe_2O_4$ Spinel Ferrite Nanocrystallites," *Journal of Physical Chemistry B*, Vol. 103, No. 33, 1999, pp. 6876-6880.doi:10.1021/jp9912307

[42] A. Sluiter, B. Hames, R. Ruiz, *et al*., "Determination of Structural Carbohydrates and Lignin in Biomass," 2008. http://www.nrel.gov/biomass/pdfs/42618.pdf

[43] A. Sluiter, B. Hames, R. Ruiz, C. Scarlata, J. Sluiter and D. Templeton, "Determination of Sugars, Byproducts, and Degradation Products in Liquid Fraction Process Samples," 2008. http://www.nrel.gov/biomass/pdfs/42623.pdf

[44] J. Silva, W. de Brito and N. Mohallem, "Influence of Heat Treatment on Cobalt Ferrite Ceramic Powders," *Materials Science Engineering B*: *Solid-State Materials for Advanced Technology*, Vol. 112, No. 2-3, 2004, pp. 182-187.

[45] M. Naseri, E. Saion, H. Ahangar, A. Shaari and M. Hashim, "Simple Synthesis and Characterization of Cobalt Ferrite Nanoparticles by a Thermal Treatment Method," *Journal of Nanomaterials*, Vol. 2010, 2010, pp. 1-8. doi:10.1155/2010/907686

[46] X. S. Zhao, G. Q. Lu and X. Hu, "Characterization of the Structural and Surface Properties of Chemically Modified MCM-41 Material," *Microporous and Mesoporous Materials*, Vol. 41, 2000, pp. 37-47.

[47] M. Colilla, I. Izquierdo-Barba, S. Sanchez-Salcedo, J. Fierro, J. Hueso and M. Vallet-Regi, "Synthesis and Characterization of Zwitterionic SBA-15 Nanostructured Materials," *Chemistry of Materials*, Vol. 22, No. 23, 2010, pp. 6459-6466. doi:10.1021/cm102827y

[48] M. Alvaro, A. Corma, D. Das, V. Fornes and H. Garcia, "Nafion-Functionalized Mesoporous MCM-41 Silica Shows High Activity and Selectivity for Carboxylic Acid Esterification and Friedel-Crafts Acylation Reactions," *Journal of Catalysis*, Vol. 231, No. 1, 2005, pp. 48-55. doi:10.1016/j.jcat.2005.01.007

[49] S. Suganuma, K. Nakajima, M. Kitano, D. Yamaguchi, H. Kato, S. Hayashi and M. Hara, "Hydrolysis of Cellulose by Amorphous Carbon Bearing SO_3H, COOH, and OH Groups," *Journal of the American Chemical Society*, Vol. 130, No. 38, 2008, pp. 12787-12793. doi:10.1021/ja803983h

[50] R. Buzzoni, S. Bordiga, G. Ricchiardi, G. Spoto and A. Zecchina, "Interaction of H_2O, CH_3OH, $(CH_3)_2O$, CH_3CN, and Pyridine with the Superacid Perfluorosulfonic Membrane Nafion: An IR and Raman Study," *Journal of Physical Chemistry*, Vol. 99, No. 31, 1995, pp. 11937-11951. doi:10.1021/j100031a023

[51] G. Blanco Brieva, J. Campos Martin, M. de Frutos and J. Fierro, "Preparation, Characterization, and Acidity Evaluation of Perfluorosulfonic Acid-Functionalized Silica Catalysts," *Industrial Engineering Chemistry Research*, Vol. 47, No. 21, 2008, pp. 8005-8010.doi:10.1021/ie800221f

[52] T. H. Kim, Y. H. Im and Y. B. Hahn, "Plasma Enhanced Chemical Vapor Deposition of Low Dielectric Constant SiCFO Thin Films," *Chemical Physics Letters*, Vol. 368, No. 1-2, 2003, pp. 36-40. doi:10.1016/S0009-2614(02)01715-3

[53] J. Scaranto, A. P. Charmet and S. Giorgianni, "IR Spectroscopy and Quantum-Mechanical Studies of the Adsorption of CH_2CClF on TiO_2," *Journal of Physical Chemistry* C, Vol. 112, No. 25, 2008, pp. 9443-9447. doi:10.1021/jp801075n

[54] C. Biloiu, I. A. Biloiu, Y. Sakai, Y. Suda and A. Ohta, "Amorphous Fluorocarbon Polymer (*a*-C: F) Films Obtained by Plasma Enhanced Chemical Vapor Deposition from Perfluoro-Octane (C_8F_{18}) Vapor I: Deposition, Morphology, Structural and Chemical Properties," *Journal of Vacuum Science & Technology A*, Vol. 22, No. 4, 2004, pp. 1158-1165. doi:10.1116/1.1759354

[55] K. Zavadil, N. Armstrong and C. Peden, "Reactions at the Interface between Multi-Component Glasses and Metallic Lithium Films," *Journal of Materials Research*, Vol. 4, No. 4, 1989, pp. 978-989. doi:10.1557/JMR.1989.0978

[56] K. Senapati, C. Borgohain and P. Phukan, "Synthesis of Highly Stable $CoFe_2O_4$ Nanoparticles and Their Use as Magnetically Separable Catalyst for Knoevenagel Reaction in Aqueous Medium," *Journal of Molecular Catalysis A*, Vol. 339, No. 1-2, 2011, pp. 24-31. doi:10.1016/j.molcata.2011.02.007

[57] S. Hamoudi, S. Royer and S. Kaliaguine, "Propyl- and Arene-Sulfonic Acid Functionalized Periodic Mesoporous Organosilicas," *Microporous and Mesoporous Materials*, Vol. 71, No. 1-3, 2004, pp. 17-25. doi:10.1016/j.micromeso.2004.03.009

[58] F. Carvalheiro, L. Duarte, R. Medeiros and F. Girio, "Optimization of Brewery's Spent Grain Dilute-Acid Hydrolysis for the Production of Pentose-Rich Culture Media," *Applied Biochemistry and Biotechnology*, Vol. 113, 2004, pp. 1059-1072. doi:10.1385/ABAB:115:1-3:1059

[59] S. E. Jacobsen and C. E. Wyman, "Xylose Monomer and Oligomer Yields for Uncatalyzed Hydrolysis of Sugarcane Bagasse Hemicellulose at Varying Solids Concentration," *Industrial Engineering Chemistry Research*, Vol. 41, No. 6, 2002, pp. 1454-1461. doi:10.1021/ie001025+

[60] C. E. Wyman, B. E. Dale, R. T. Elander, M. Holtzapple, M. R. Ladisch and Y. Y. Lee, "Coordinated Development of Leading Biomass Pretreatment Technologies," *Bioresource Technology*, Vol. 96, No. 18, 2005, pp. 1959-1966. doi:10.1016/j.biortech.2005.01.010

[61] S. Allen, D. Schulman, J. Lichwa, M. Antal and E. Jennings, "A Comparison of Aqueous and Dilute-Acid Single-Temperature Pretreatment of Yellow Poplar Sawdust," *Industrial Engineering Chemistry Research*, Vol. 40, No. 10, 2001, pp. 2352-2361. doi:10.1021/ie000579+

[62] T. Marzialetti, C. Sievers and P. Agrawal, "Dilute Acid

Hydrolysis of Loblolly Pine: A Comprehensive Approach," *Industrial Engineering Chemistry Research*, Vol. 47, No. 19, 2008, pp. 7131-7140. doi:10.1021/ie800455f

[63] A. Corma, S. Iborra and A. Velty, "Chemical Routes for the Transformation of Biomass into Chemicals," *Chemical Reviews*, Vol. 107, No. 6, 2007, pp. 2411-2502. doi:10.1021/cr050989d

[64] B. Girisuta, L. Janssen and H. Heeres, "A Kinetic Study on the Conversion of Glucose to Levulinic Acid," *Chemical Engineering Research and Design*, Vol. 84, No. 5, 2006, pp. 339-349. doi:10.1205/cherd05038

[65] G. Bonn and O. Bobleter, "Determination of the Hydrothermal Degradation Products of D-(U-^{14}C) Glucose and D-(U-^{14}C) Fructose by TLC," *Journal of Radioanalytical Chemistry*, Vol. 79, No. 2, 1983, pp. 171-177. doi:10.1007/BF02518929

[66] A. P. Dunlop, "Furfural Formation and Behavior," *Industrial Engineering Chemistry*, Vol. 40, No. 2, 1948, pp. 204-209. doi:10.1021/ie50458a006

[67] M. J. Antal, T. Leesomboon, W. S. Mok and G. N. Richards, "Mechanism of Formation of 2-Furaldehyde from D-Xylose," *Carbohydrate Research*, Vol. 217, 1991, pp. 71-85. doi:10.1016/0008-6215(91)84118-X

[68] F. Carrasco and C. Roy, "Kinetic-Study of Dilute-Acid Prehydrolysis of Xylan-Containing Biomass," *Wood Science and Technology*, Vol. 26, No. 3, 1992, pp. 189-208. doi:10.1007/BF00224292

[69] R. Torget and T. Hsu, "Two-Temperature Dilute-Acid Prehydrolysis of Hardwood Xylan Using a Percolation Process," *Applied Biochemistry and Biotechnology*, Vol. 45-46, 1994, pp. 5-21. doi:10.1007/BF02941784

[70] S. B. Kim, Y. Y. Lee and R. Torget, "Kinetics in Acid-Catalyzed Hydrolysis of Hardwood Hemicellulose," *Biotechnology & Bioengineering Symposium*, Vol. 17, 1987, pp. 71-84.

[71] K. Grohmann, R. Torget and M. Himmel, "Optimization of Dilute Acid Pretreatment of Biomass," *Biotechnology & Bioengineering Symposium*, Vol. 15, 1986, pp. 59-80.

[72] C. Liu and C. E. Wyman, "Effect of the Flow Rate of a Very Dilute Sulfuric Acid on Xylan, Lignin, and Total Mass Removal from Corn Stover," *Industrial & Engineering Chemistry Research*, Vol. 43, No. 11, 2004, pp. 2781-2788. doi:10.1021/ie030754x

[73] J. Grondin, R. Sagnes and A. Commeyras, "Perfluorosulfonic Acids-3. Hammett Acidity Functions of Perfluoroalkanesulfonic Acids and of their Mixtures with SbF5," *Bulletin de la Société Chimique de France*, No. 11, 1976, pp. 1779-1783.

[74] A. Corma, D. Das, V. Fornes, H. Garcia and M. Alvaro, "Single-Step Preparation and Catalytic Activity of Mesoporous MCM-41 and SBA-15 Silicas Functionalized with Perfluoroalkylsulfonic Acid Groups Analogous to Nafion (R)," *Chemical Communications*, No. 8, 2004, pp. 956-957.

[75] W. M. Van Rhijn, D. E. De Vos, B. F. Sels, W. D. Bossaert and P. A. Jacobs, "Sulfonic Acid Functionalized Ordered Mesoporous Materials as Catalysts for Condensation and Esterification Reactions," *Chemical Communications Cambridge*, Vol. 1998, No. 3, 1998, pp. 317-318. doi:10.1039/a707462j

